

Ateneo de Manila University

**Archium Ateneo**

---

Environmental Science Faculty Publications

Environmental Science Department

---

1999

## Development of $^{31}\text{P}$ Nuclear Magnetic Resonance Methods for the Study of Phosphate Metabolisms in *E. coli* and *B. subtilis*

Fabian M. Dayrit

Emilyn Q. Espiritu

Noreen Gonzalez

Nina Rosario L. Rojas

Jennifer T. Aguilan

*See next page for additional authors*

Follow this and additional works at: <https://archium.ateneo.edu/es-faculty-pubs>



Part of the [Biochemistry Commons](#), and the [Molecular Biology Commons](#)

---

---

**Authors**

Fabian M. Dayrit, Emilyn Q. Espiritu, Noreen Gonzalez, Nina Rosario L. Rojas, Jennifer T. Aguilan, Antonio M. Basilio, Edward T. Chainani, Enrico Cruz, and Bernadette Matanguihan

---

## Development of $^{31}\text{P}$ Nuclear Magnetic Resonance Methods for the Study of Phosphate Metabolisms in *E. coli* and *B. subtilis*

Fabian M. Dayrit, Emilyn Q. Espiritu, Noreen Gonzalez, Nina Rojas, Jennifer T. Aguilan, Antonio M. Basilio, Edward T. Chainani, Enrico Cruz, and Bernadette Matanguihan

Department of Chemistry  
Ateneo de Manila University  
Loyola Heights, Quezon City

---

$^{31}\text{P}$  NMR experiments were performed on *Escherichia coli* and *Bacillus subtilis* at various temperatures under aerobic and anaerobic conditions. The total soluble intracellular phosphate concentration was estimated to be  $2 \times 10^{-17}$  mole/cell, while intracellular orthophosphate concentration was around  $1 \times 10^{-17}$  mole/cell. Addition of glucose resulted in a general decrease in intracellular pH and was accompanied by the formation of sugar monophosphates. The concentrations of soluble intracellular phosphates, both inorganic and organic phosphates, were estimated by integration versus methylene diphosphonic acid (MDPA) standard. Although intracellular and extracellular orthophosphate could be observed, these appear to exchange rapidly on the NMR time scale.

---

**Key words:**  $^{31}\text{P}$  NMR method, phosphate metabolism, *E. coli*, *B. subtilis*

### INTRODUCTION

Phosphorous plays an important role in biology, whether it is in the form of inorganic phosphates or metabolically important organic (biological) phosphates. Phosphorous is estimated to comprise about 0.5% of wet biomass. It is classified as a macronutrient and plays a very important role in metabolism, replication, and membrane structure.

There is considerable interest in the role of phosphorous in cellular metabolism. Phosphorous-containing compounds occur mainly as inorganic phosphates and biological organophosphates. Inorganic phosphates are found in the biological cell as orthophosphate or polyphosphates. Biological organophosphate derivatives are generally attached to sugars (for example, glucose phosphates), nucleotide sugars (for example, ATP and DNA), alcohols (for example, phosphoenol pyruvate), carboxylic acids (for example, acetyl phosphate), and lipids (phospholipids). Other less common biological phosphorous compounds include: phosphonates (phosphonic acid derivatives) and phosphodiester (cyclic phosphates).

It is well known that bacteria continuously adapt to their environment. For example, the presence of  $\text{O}_2$  has been shown to regulate cellular metabolism in facultative anaero-

bic bacteria, such as *E. coli*, where a great variety of genes are activated positively or negatively [1]. One of the elements for which bacteria have developed a high sensitivity for is phosphorous. It has been found that the phosphate equilibrium in *E. coli* is regulated by  $P_i$  input from the surrounding medium [2-4].

By the very complex chemical nature of biological systems, it is often difficult to carry out direct spectroscopic measurements of the cell. However, by taking advantage of the ability of NMR to selectively observe specific nuclei, it is possible to understand biochemical processes in greater detail [5]. The ability to study phosphorous metabolism *in vivo* has become an important research tool. In 1973, Moon and Richards pioneered the use of  $^{31}\text{P}$  NMR for the study of metabolism in whole rabbit blood. They observed signals due to inorganic phosphate and a number of organic phosphates such as 2,3-diphosphoglyceric acid, phospholipids, and ATP. A wide range of biological samples have been studied by  $^{31}\text{P}$  NMR, including bacteria [6], algae [7-8], plant cells [9], immobilized cells [10], isolated organs and whole animals [11]. NMR is now considered as a valuable and unique method for the study of metabolism in biology.

The  $^{31}\text{P}$  NMR method has a number of unique features, which make it particularly attractive for the study of metabolism in microorganisms. Because NMR is non-destructive, cells can

be observed as they are actively metabolizing. Thus, dynamic cellular processes can be observed. Only soluble phosphorous compounds are observed, such as inorganic phosphates (orthophosphate and polyphosphates) and low-molecular weight organic phosphates. Signals from macromolecules, such as, cell wall immobilized phospholipids, phosphates in DNA, etc., are not observed.

There are, however, a number of limitations of the  $^{31}\text{P}$  NMR methodology. Because NMR is an inherently insensitive technique, a high concentration of cells is needed to obtain good signals. If a high cell concentration is not possible, a larger number of scans may be accumulated but the disadvantage is the need for longer experiment time and the corresponding poorer time resolution (time-averaged spectra). There are a number of conditions *in vivo* that tend to complicate the NMR signal, such as the dynamic flow of compounds in the cell and the possibility that mobility of compounds is less than would be observed in an ideal solution. As a result, the line widths of  $^{31}\text{P}$  signals in bacteria are wide resulting in poorer resolution of  $^{31}\text{P}$  signals, and severe overlap of signals. Despite these difficulties,  $^{31}\text{P}$  NMR offers a unique and powerful approach for the observation compounds in microorganisms *in vivo*.

In this paper, we report on the development of a method for the study of phosphorous metabolism in microorganisms (*E. coli* and *B. subtilis*) using  $^{31}\text{P}$  NMR.

## EXPERIMENTAL

**Strains.** *E. coli* UPCC195 and *B. subtilis* were obtained from UP Culture Collection, UP Diliman. The organisms were maintained at 4°C on slants containing Luria-Bertani (LB) agar.

**Media and Growth.** The bacteria were inoculated aseptically into 1200 mL LB broth and were grown at 37°C, aerated by shaking at 80 rpm for 18 hours. The culture was then cooled in an ice bath. The cells were harvested by centrifugation for 5 minutes at 6°C and were washed twice with an equal volume of phosphate buffer (10mM  $\text{Na}_2\text{HPO}_4$ , 10mM  $\text{KH}_2\text{PO}_4$ , 50mM MES, 50 mM Tris, 85mM NaCl at pH 7.3). The cells were then resuspended in the same phosphate buffer medium. The cell concentration was determined by reading optical density (OD) at 600 nm, at which wavelength 1 OD unit corresponds to  $0.8 \times 10^9$  cells/mL.

Alternatively, cells were resuspended using any of the following three variations: distilled water; Tris-HCl; 8.5mM NaCl, 18.7 mM  $\text{NH}_4\text{Cl}$ , 0.1 mM  $\text{CaCl}_2$ , and 10mM  $\text{MgCl}_2$ .

**NMR: General.** NMR experiments were performed using a JEOL Lambda 400 (9.4 tesla magnetic field) with a standard 54 mm bore and a 10-mm tunable probe.  $^{31}\text{P}$  were observed at 161.70 MHz. The bacteriae suspension were placed in a 10-mm NMR tube. Spectra were taken in the non-spin-

ning mode. Two pulse programs were used: a single pulse mode (identical to a standard  $^1\text{H}$  measurement) and a  $^1\text{H}$ -broadband decoupled single pulse mode (identical to a standard  $^{13}\text{C}$  measurement). Spectral width was about 20 kHz and the number of data points was 1024 which was zero-filled to 2048 giving a spectral resolution of about 10 Hz. The pulse angle used was 67°, with a pulse delay of 3 seconds. The purpose of the relatively longer pulse delay was to ensure that the magnetization of the MDPA standard is fully relaxed between scans. The number of accumulations varied from 70 to 500 times, with a total accumulation time of 3.5 to 10 minutes. FIDs were processed using an exponential window with a line broadening of 10 Hz.

**NMR:  $^{31}\text{P}$  Reference.** The phosphorous reference and deuterium lock were provided by dissolving methylene diphosphonic acid (MDPA, 0.54 M or 0.10 M) in  $\text{D}_2\text{O}$  or methanol- $\text{D}_4$  and placing this solution inside a capillary which was held in place in the center of the 10-mm NMR tube a Teflon plug which had a hole drilled in the center. The chemical shift position of MDPA was experimentally determined to be +18.97 ppm vs. 85%  $\text{H}_3\text{PO}_4$ .

**NMR:  $^{31}\text{P}$  Standards.** The following phosphate standards were made up to a final concentration of 10 mM in the 10-mm NMR tube: ATP, ADP, AMP, glucose-1-phosphate, orthophosphate, and polyphosphate.

**NMR: pH versus  $^{31}\text{P}$  Chemical Shift.** Nine  $\text{KH}_2\text{PO}_4$  solutions, each about 20 mM, were prepared. The pH values of the phosphate solutions were adjusted by addition of NaOH (1.0 M) at room temperature and the pH was measured with a pH meter. The  $^{31}\text{P}$  NMR spectrum of each solution was determined at 8°, 20° and 29°C vs. MDPA.

**$^{31}\text{P}$  NMR Analysis of Bacteria.** The bacterial cells were filtered, washed thrice and resuspended in ca. 5 mL in the appropriate medium and then transferred to the 10-mm NMR tube. The bacteria were kept in an ice-bath during this entire procedure. The NMR experiments were started as soon as possible to minimize aging of the bacteria. Experiments were carried out at various temperatures as indicated in the individual experiments. The atmospheric condition in the 10-mm *nmr* tube was controlled by bubbling filtered  $\text{N}_2$  or air (Fig. 1.)

## RESULTS AND DISCUSSION

**Experimental Determination of  $^{31}\text{P}$  Chemical Shift of Orthophosphate versus pH.** In principle, all ionizable phosphates exhibit a pH dependence in their  $^{31}\text{P}$  chemical shift because of acid-base equilibria. The chemical shifts ( $^{31}\text{P}$ , ppm) of orthophosphate were measured from pH 4.64 to 9.00 at around 0.5 pH unit intervals. The pH conditions and observed  $^{31}\text{P}$  chemical shift positions are plotted in Figure 2. The plots of pH versus  $^{31}\text{P}$  chemical shift at the three different temperatures all show very similar sigmoidal curves. The

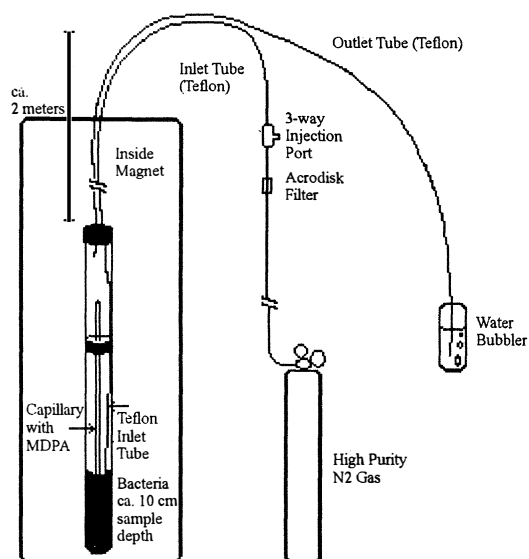


Fig. 1. Illustration of the 10-mm NMR tube with attachments for addition of reagents and bubbling of nitrogen or air. The temperature of the sample culture in the probe was within  $\pm 0.1^\circ\text{C}$  of the temperature setting.

differences in  $^{31}\text{P}$  chemical shift ranged from 0.0 ppm to 0.13 ppm. This indicates that there is a small dependence of the pH on temperature.

The maximum slope was obtained from pH 6 to 8. Since this is the range of pH values expected for biological systems, this makes the chemical shift of inorganic phosphate specially suited for the determination of the pH of biological systems. The following curve-fitting equation for a sigmoidal curve was obtained:

$$\left\{ \ln \left( \frac{(-2.36686)}{(\delta - 3.0411)} - 1 \right) \times 0.45206 \right\} + 7.0750 = \text{pH}(\text{calc})$$

Equation 1

Alternatively, if one knows the pH of the solution, one can calculate the  $^{31}\text{P}$  chemical shift,  $\delta$ :

$$\left\{ \frac{(-2.36686)}{\left[ \exp \left( \frac{\text{pH} - 7.0750}{0.45206} \right) + 1 \right]} \right\} + 3.0411 = \delta(\text{calc})$$

Equation 2

An exponential line-broadening factor of 10 Hz was applied to the  $^{31}\text{P}$  spectra to decrease the noise in the spectra. This gives an uncertainty of  $\pm 0.062$  ppm in the position of the  $^{31}\text{P}$  peaks. This contributes an uncertainty of about 0.05 pH unit. In practice, because of the broadness of the  $^{31}\text{P}$  signals in the bacterial sample and the 10 Hz line broadening used, the precision is  $\pm 0.1$  pH unit [12].

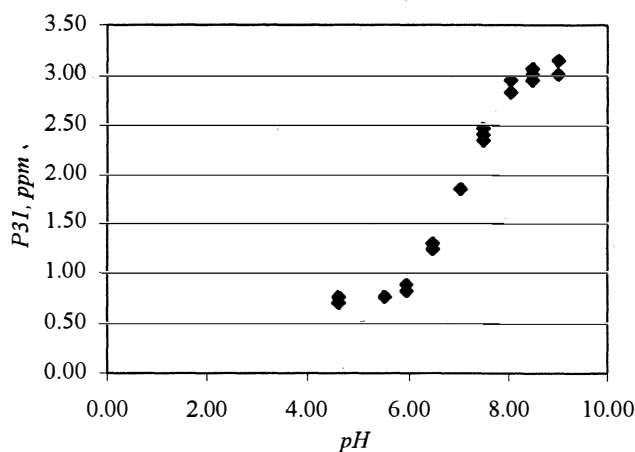


Fig. 2. Plot of experimental  $^{31}\text{P}$  chemical shift of orthophosphate vs. pH at  $8^\circ$ ,  $20^\circ$ , and  $29^\circ$ .

**Organic Phosphates: pH Dependence of  $^{31}\text{P}$  Chemical Shift.** A cell contains numerous phosphorous-containing metabolites. These include organic phosphates ( $\text{ROPO}_3^{-2}$ ), organic diphosphates ( $\text{ROPO}_2\text{-OPO}_3^{-3}$ ), organic triphosphates diphosphates ( $\text{ROPO}_2\text{-OPO}_2\text{-OPO}_3^{-4}$ ), and organic phosphonates ( $\text{RPO}_3^{-2}$ ). These organic phosphates exhibit pH dependence because they are ionizable (*i.e.*, they possess  $K_a$  values). In addition, the diphosphates and triphosphates (*e.g.*, ADP, and ATP) may exhibit chemical shift effects due to the presence of chelating cations such as  $\text{Mg}^{+2}$  or  $\text{Ca}^{+2}$  [13].

It is necessary determine the chemical shifts of such compounds in order to assign the signals obtained in the  $^{31}\text{P}$  NMR spectrum of bacterial cultures. Table 1 shows the chemical shifts of the following compounds in water and in the presence of  $\text{Mg}^{+2}$ : ATP, ADP, AMP, glucose-1-phosphate, and orthophosphate.

Table 2 summarizes the changes in  $^{31}\text{P}$  chemical shifts for the phosphorous nuclei in ATP, ADP, AMP, glucose-1-phosphate, and orthophosphate ( $\text{P}_i$ ) between  $8^\circ\text{C}$  and  $25^\circ\text{C}$  un-

**Table 1. Experimental  $^{31}\text{P}$  assignments of organic phosphates in water at  $25^\circ\text{C}$  and upon addition of  $\text{MgCl}_2$ . Chemical shifts are referenced versus MDPA. Chemical shifts are rounded off to the nearest 0.1 ppm unit.**

Phosphate compound	$^{31}\text{P}$ , ppm	$^{31}\text{P}$ , ppm (+ $\text{MgCl}_2$ )	Difference ppm
ATP, $\beta$	-22.4	-21.6	+0.8
$\alpha$	-10.7	-10.6	+0.1
$\gamma$	-10.1	-10.0	+0.1
ADP, $\alpha$	-10.5	-10.5	0.0
$\beta$	-10.0	-9.7	+0.3
AMP	0.9	0.9	0.0
G-1P	-0.6	-0.6	0.0

**Table 2. Differences in  $^{31}\text{P}$  chemical shifts at  $8^\circ\text{C}$  and  $25^\circ\text{C}$  under various pH conditions, in 5 mM  $\text{Mg}^{2+}$ :  $\delta(25^\circ\text{C}) - \delta(8^\circ\text{C})$ . Chemical shifts are rounded off to the nearest 0.1 ppm.**

Phosphate	Differences in $^{31}\text{P}$ chemical shift, ppm, between $8^\circ\text{C}$ and $25^\circ\text{C}$ in the presence of 5 mM $\text{MgCl}_2$			
	pH = 4.3	pH = 5.2*	pH = 6.3*	pH = 7.8*
ATP, $\beta$	+0.1	+0.2	0.0	0.0
$\alpha$	0.0	0.0	+0.1	+0.1
$\gamma$	-0.1	-0.1	0.0	+0.1
ADP, $\alpha$	0.0	0.0	+0.1	+0.1
$\beta$	-0.4	-0.1	0.0	+0.1
AMP	0.0	-0.1	0.0	0.0
G-1P	-0.1	-0.1	0.0	+0.1
$\text{P}_i$	0.0	0.0	0.0	+0.1

\*pH calculated from chemical shift of inorganic phosphate,  $\text{P}_i$ , using equation 1.

der various pH conditions, in 5 mM  $\text{Mg}^{2+}$ . The biggest effect of the addition of  $\text{Mg}^{2+}$  is observed in the  $\beta$  phosphate of ATP. This is consistent with previous observations on the effect of added salts on  $^{31}\text{P}$  chemical shifts of various phosphates in nucleic acids [13]. Only minor changes in chemical shift were observed for ADP, AMP, glucose-1-phosphate, and orthophosphate. Data obtained from various experiments also show that temperature does not have a significant effect on  $^{31}\text{P}$  chemical shift.

Robitaille and co-workers [12] determined the pH-dependent chemical shift behavior of a large number of phosphorous-containing metabolites, including inorganic phosphate, phosphomonoesters (e.g., sugar monophosphates), phosphodiester (e.g., sugar diphosphates), and nucleotide phosphates (e.g., ATP, ADP, and AMP). Assuming a single  $pK_a$  [ $\text{HA} \rightarrow \text{H}^+ + \text{A}^-$ ], they proposed the following equation:

$$\frac{\{\delta_1 + (\delta_2 \times 10^{(pH-pK_a)})\}}{\{10^{(pH-pK_a)} + 1\}} = \delta(\text{calc})$$

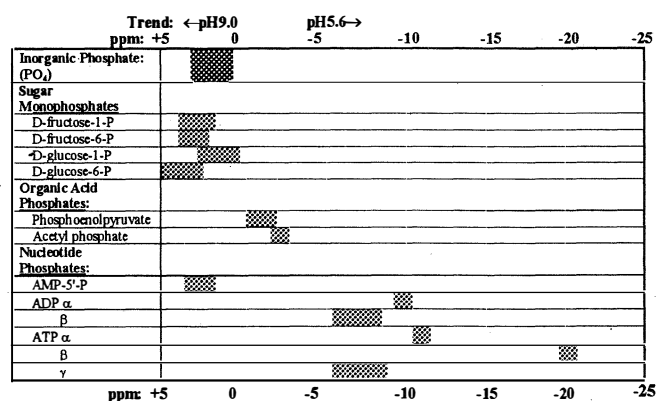
Equation 3

where:  $\delta_{\text{calc}}$  is the calculated  $^{31}\text{P}$  chemical shift (in ppm) of the phosphate compound at the pH of the solution,  $\delta_1$  and  $\delta_2$  are the chemical shifts of the acid and conjugate base, respectively, and  $pK_a$  is the acid dissociation constant. Equation 3 can be rearranged into the following form:

$$pK_a + \log \frac{[\delta_{\text{obs}} - \delta_1]}{[\delta_2 - \delta_{\text{obs}}]} = pH(\text{calc})$$

Equation 4

Table 3 presents some of the experimental values for  $\delta_1$ ,  $\delta_2$ , and  $pK_a$  which were given by Robitaille and co-workers [12]. We can compare our own experimental results with those of



**Fig. 3. Range of  $^{31}\text{P}$  chemical shift values (ppm) for the various phosphorous compounds within the pH range 9.0 to 5.6. Chemical shifts were calculated from Robitaille and co-workers [12] and our standard values.**

Robitaille, et al. by using equation 3 to generate a pH vs. chemical shift plot for inorganic phosphate,  $\text{P}_i$ . In general, our experimental data agree well with literature values. Figure 3 gives the range of expected values for the various metabolic phosphates within the pH range 9.0 to 5.6.

**Quantitation of Inorganic Phosphate versus MDPA Standard.** Using the known concentration of the MDPA standard (0.54 M or 0.10 M); it is possible to estimate the concentrations of the various phosphates in the biological sample. However, the accuracy of this method is limited by the following:

- **Mobility of the Compound.** The relaxation time of the nucleus is determined by its NMR correlation time, a condition that is related to the mobility of the compound in solu-

**Table 3. Table of values used for the calculation of  $^{31}\text{P}$  chemical shift of organophosphates under various pH conditions using equations 3 and 4 [12].**

Compound	$\delta_1$	$\delta_2$	$pK_1$
Dihydrogenphosphate ( $\text{H}_2\text{PO}_4^-$ )	0.66	3.18	7.05
Acetyl phosphate	-6.30	-1.54	4.68
D-fructose-1-P	0.67	4.15	5.92
D-fructose-6-P	1.09	4.46	6.06
D-glucose-1-P	-0.57	3.00	6.04
D-glucose-6-P	1.35	5.03	6.03
Phosphoenol pyruvate	-3.61	0.01	5.74
AMP-5'-P	0.87	4.41	6.11
ADP, $\alpha$	-10.45	-9.69	6.00
$\beta$	-9.88	-5.36	6.03
ATP, $\alpha$	-10.59	-10.16	5.61
$\beta$	-21.91	-20.38	5.77
$\gamma$	-9.88	5.11	5.97

tion. Compounds which have a high molecular weight, or those which are partially aggregated or attached to macromolecules give erroneous integration or may not be detectable by NMR. On the other hand, mobile small molecular weight compounds can be quantified by integration.

- **NMR Relaxation Time.** In order to ensure accuracy of the integration, in particular for a heterogeneous sample such as biological systems, the pulse delay should be set to ensure complete relaxation of both the rapidly relaxing and slowly relaxing constituents. In our system, the pulse delay was set to 3.0 seconds to ensure relaxation of the MDPA reference.

- **NMR Exchange.** Rapidly exchanging sites yield an averaged spectrum and can result in broadened peak shapes. This leads to inaccuracies in integration.

- The accuracy and precision of NMR integration is directly dependent on the signal-to-noise ratio. In metabolizing biological systems, signal-to-noise is sometimes a major limitation.

- In biological systems, the accuracy of integration is limited by overlap of  $^{31}\text{P}$  signals.

**$^{31}\text{P}$  NMR Spectra of *E. coli* and *B. subtilis*.** Because of the inherent low sensitivity of NMR, the bacterial cells have to be present at concentration higher than what is normally obtained in a suspension culture ( $>10^{11}$  cells/mL). This is over 100 times more concentrated than the usual cell suspension culture. Therefore, it was necessary to develop the procedures to prepare the bacterial sample at such high cell density, and at the same time ensuring that the bacteria are in the proper phase of growth.

Figures 4 and 5 are typical examples of the  $^{31}\text{P}$  NMR spectra. The  $^{31}\text{P}$  chemical shift of orthophosphate,  $\text{P}_i$ , is used to determine pH. The precision of the pH correlation is  $\pm 0.1$  pH unit. The integration is based on the signal of the reference (MDPA) being assigned as 100%. The integration values have a precision of  $\pm 10\%$ .

Figure 4a shows that the  $^{31}\text{P}$  NMR spectra of *E. coli* do not vary significantly from 8 to  $37^\circ\text{C}$ . Upon addition of  $\text{KH}_2\text{PO}_4$  (Figure 4b, middle spectrum), the spectrum broadens and two major peaks are observed. These are assigned to  $\text{P}_i(\text{in})$  and  $\text{P}_i(\text{out})$ . The pH values inside and outside the cell are 7.9 and 7.2, respectively. Upon standing (Fig. 4b, bottom spectrum), the orthophosphate peaks coalesce.

Figure 5 shows the  $^{31}\text{P}$  NMR spectra of *B. subtilis* at  $15^\circ\text{C}$ . Addition of glucose significantly increases the amount of sugar phosphate in the cell (compare top and middle spectra). Addition of  $\text{KH}_2\text{PO}_4$ , however, did not give two separate orthophosphate signals, indicating that exchange of inside and outside orthophosphate is rapid.

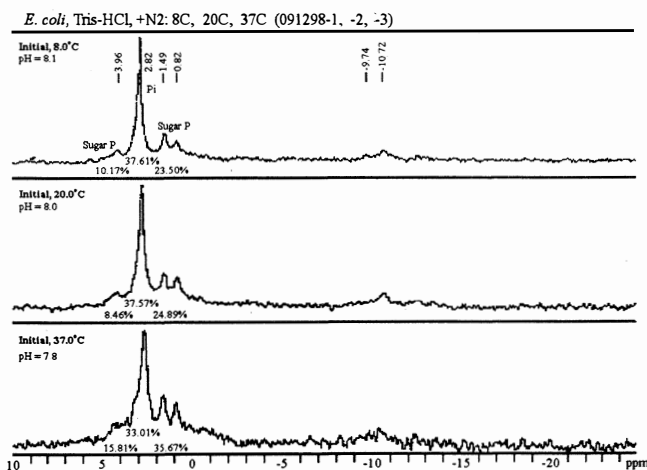


Fig. 4a. *E. coli* cell density:  $4.13 \times 10^{11}$ , MDPA: 0.54 M. Conditions:  $\text{N}_2$  bubbled into NMR tube, used Tris-HCl buffer, no phosphate buffer. (run: 091298)  
Top:  $^{31}\text{P}$  NMR spectrum at initial culture conditions,  $8.0^\circ\text{C}$ . Cellular pH is 8.0.  
Middle: Spectrum after culture is warmed to  $20.0^\circ\text{C}$ . Cellular pH is 8.0.  
Bottom: Spectrum after culture is warmed to  $37.0^\circ\text{C}$ . Cellular pH is 7.8.

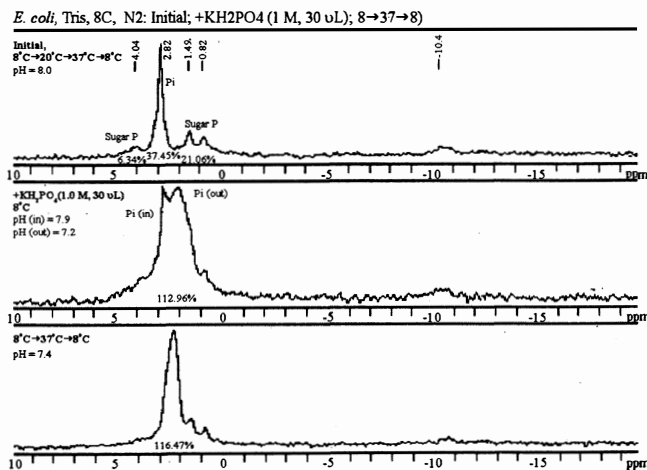


Fig. 4b. *E. coli* cell density:  $4.13 \times 10^{11}$ , MDPA: 0.54 M. Conditions:  $\text{N}_2$  bubbled into NMR tube, used Tris-HCl buffer, no phosphate buffer. (run: 091298) Continued from Figure 4a.  
Top:  $^{31}\text{P}$  NMR spectrum after cycling the temperature:  $8 \rightarrow 20 \rightarrow 37 \rightarrow 8^\circ\text{C}$ . Cellular pH is 8.0.  
Middle: Spectrum after addition of  $30 \mu\text{L}$  of 1.0 M  $\text{KH}_2\text{PO}_4$  at  $8.0^\circ\text{C}$ . Two  $\text{P}_i$  peaks are observed: inside and outside. Cellular pH is 7.9; external pH is 7.2.  
Bottom: Spectrum after culture is warmed to  $37^\circ\text{C}$  and recooled to  $8^\circ\text{C}$ . The two orthophosphate signals have coalesced. Average pH is 7.4.

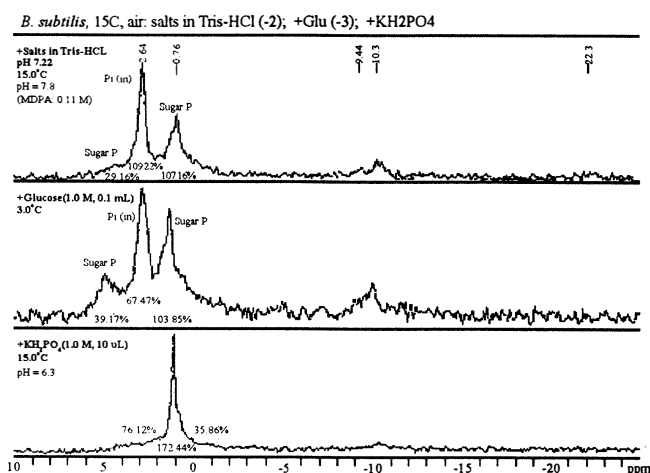


Fig. 5. *B. subtilis* cell density:  $1.78 \times 10^{11}$ , MDPA: 0.10 M. Conditions: Air bubbled into NMR tube, used Tris-HCl buffer, no phosphate buffer. (run: 020999) Top:  $^{31}\text{P}$  NMR spectrum of culture at initial conditions. Temperature:  $15.0^\circ\text{C}$ . Cellular pH is 7.8. Middle: Spectrum after addition of  $100 \mu\text{L}$  of 1.0 M glucose at  $15.0^\circ\text{C}$ . Bottom: Spectrum after addition of  $10 \mu\text{L}$  of 1.0 M  $\text{KH}_2\text{PO}_4$  at  $15.0^\circ\text{C}$ . Only one orthophosphate peak is observed. Average pH is 6.3.

A number of observations can be made from the various  $^{31}\text{P}$  NMR experiments:

1.  $P_i$  (in) and  $P_i$  (out) can be observed at a sufficiently low temperature, but if allowed to stand, the two signals merge due to exchange giving only one observed  $^{31}\text{P}$  signal for  $P_i$ . However, if the system is allowed to equilibrate, the two peaks coalesce. This suggests that equilibration between  $P_i$  (in) and  $P_i$  (out) is occurring which is rapid on the *nmr* time scale giving only one averaged  $^{31}\text{P}$  signal for  $P_i$ .
2. Under aerobic conditions, a relatively larger concentration of organic phosphates is observed.
3. Upon addition of glucose, there was a significant increase observed in the intensity of signals centered around 4.89 and 1.24 ppm assignable to sugar monophosphates.

Table 4. Preliminary estimate of the concentration of intracellular phosphorous as total phosphorous and inorganic orthophosphate,  $P_i$ . Estimates are made for initial bacterial samples in phosphate-deficient media.

Experiment	Integration vs. MDPA		P concentration M, (calc)		Cell density (cells/mL)	Soluble P mole/cell (calc)	
	$P(\text{total})$	$PO_4$	$P(\text{total})$	$[P_i]$		$P(\text{total})$	$P_i$
<i>E. coli</i>							
082998	95.6	57.06	0.0069	0.0041	$4.1\text{E}+11$	$1.7\text{E}-17$	$1.0\text{E}-17$
091298	80.09	37.61	0.0058	0.0027	$4.1\text{E}+11$	$1.4\text{E}-17$	$6.6\text{E}-18$
112698	61.36		0.0044		$4.0\text{E}+11$	$1.1\text{E}-17$	
<i>B. subtilis</i>							
020999	279.05	109.22	0.0041	0.0016	$1.8\text{E}+11$	$2.3\text{E}-17$	$9.0\text{E}-18$

**Concentration of Soluble Intracellular Phosphates.** The concentration of soluble intracellular phosphates can be estimated from the integration of the various  $^{31}\text{P}$  signals and the cell concentration (cells/mL) under initial conditions under phosphate-deficient conditions (Table 4). Preliminary data obtained from these experiments indicate that the concentrations of total soluble phosphorous compounds and orthophosphate are about 0.006 M and 0.004 M, respectively. Using the data on cell density, the estimated concentration of total mole phosphorous per cell and total mole orthophosphate per cell are  $2 \times 10^{-17}$  and  $1 \times 10^{-17}$ , respectively. These estimates are order-of-magnitude figures and they are dependent on the conditions of the experiment. For comparison, the intracellular solution of the mammalian cell has been reported to have a  $P_i$  concentration of 0.05 M [14].

## CONCLUSION

NMR is a unique method for studying various metabolic characteristics of the cell *in vivo*.  $^{31}\text{P}$  NMR, in particular, offers a facile way of determining intracellular pH and for measuring the concentration of soluble phosphorous-containing cellular components. The major observations from this work are summarized as follows:

1. In *E. coli* and *B. subtilis*, the concentration of total soluble phosphorous compounds and orthophosphate are about  $2 \times 10^{-17}$  and  $1 \times 10^{-17}$  mole per cell, respectively.
2. Addition of glucose to the culture causes a decrease in cell pH and an increase in sugar monophosphates. At  $3.0^\circ\text{C}$  and below, glucose metabolism is very slow; no increase in signal of sugar monophosphate is observed.
3. Immediately after addition of  $\text{KH}_2\text{PO}_4$  to a phosphate-deficient medium, two orthophosphate signals can sometimes be observed; these are assigned to  $P_{i(\text{in})}$  and  $P_{i(\text{out})}$ . If the system is allowed to stand, the two peaks coalesce indicating rapid exchange of  $P_{i(\text{in})}$  and  $P_{i(\text{out})}$ . Under conditions where both peaks are observed, the exchange rate is estimated to be around  $1 \times 10^2 \text{ s}^{-1}$ . Under conditions of rapid exchange, the exchange rate is estimated to be greater than  $6 \times 10^3 \text{ s}^{-1}$ .



The results reported in this paper clearly demonstrate the unique potential that NMR has for studying biochemical processes *in vivo*.

## ACKNOWLEDGEMENT

This research was funded by the Philippine Council for Advanced Science and Technology Research and Development, Department of Science and Technology (PCASTRD, DOST).








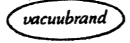





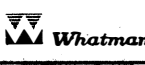







## REFERENCES

1. Uden, G. and Trageser, M. *Antonie Van Leeuwenhoek*. 59, 65 (1991).
2. Stock, J.B., Ninfa, A.J., and Stock, A.M. *Microbiol Rev*. 53, 450 (1989).
3. Scarlato, V., Arico, B., Domenighini, M., and Rappuoli, R. *Bioessays*. 15, 99 (1993).
4. Scholten, M., Janssen, R., Bogaarts, C., van Strien, J., and J. Tommassen. *J. Mol Microbiol*. 15, 247 (1995).
5. Markley, J.L. and Opella, S.J. (editors). *Biological nmr Spectroscopy*. (Oxford University Press, NY, 1997).
6. Ugurbil, K., Shulman, R.G., and Brown, T.R. In *Biological Applications of Magnetic Resonance*. (Ed. by R.G. Shulman). Acad. Press, NY (1979).
7. Mitsumori, F. and Ito, O. *FEBS Lett*. 174, 248 (1984).
8. Sianoudis, J., Küsel, A.C., Naujokat, T., Offermann, W., Mayer, A., Grimme, L.H., and Leibfritz, D. *Eur. Biophys. J*. 13, 89 (1985).
9. Wray, V., Schiel, O., Berlin, J., and Witte, L. *Arch. Biochem. Biophys*. 236, 731 (1985).
10. Vogel, H.J., Brodelius, P., Lilja, H., and Lohmeier-Vogel, E.M. *Methods in Enzymology*, Vol. 135. Acad. Press, Inc., NY, (1987).
11. Cohen, S.M. (editor). *Physiological nmr Spectroscopy: From Isolated Cells to Man*, Vol. 508, Ann. NY Acad. Sci., NY (1987).
12. Robitaille, P.M.L., Robitaille, P.A., Brown Jr., G.G., and Brown, G. G. *J. Magn. Reson.* 92, 73 (1991).
13. Roberts, J. In *Nuclear Magnetic Resonance*. (Ed. by H.F. Linskens and J.F. Jackson). Springer-Verlag, Berlin (1986).
14. Brock, T.D., Smith, D.W., and Madigan, M.T. *Biology of Microorganisms*, 4<sup>th</sup> edition. Prentice-Hall, N.J. (1984).



## GOLDEN BAT (FAR EAST) INC.

SCIENTIFIC APPARATUS, INSTRUMENTS & SUPPLIES  
FOR: INDUSTRIAL, EDUCATIONAL, CLINICAL, HOSPITAL, & RESEARCH LABORATORIES

 WATER STILLS, SHAKING, TEMPERING, INCUBATING EQUIPMENT	 CONSOLIDATED STILLS & STERILIZERS	 CSC SCIENTIFIC COMPANY, INC.	 WHEATON SCIENCE PRODUCTS A DIVISION OF AM LAWSON MARSH WHEATON	 PRECISION - PIPET TIPS / PCR TUBE	 Soil Testing Equipment	 SPECIALISTS IN THE MEASUREMENT AND CONTROL OF VISCOSITY	 SPECIALIZED IN ALL VACUUM PUMPS STD/CHEMISTRY DESIGN, VACUUM GAUGES & ACCESSORIES
 HEATING, CONTROL, SHAKING, VORTEXING, ROTATING, STIRRING, HOMOGENIZING & S. STEEL LAB. PEGBOARD	 CONSTRUCTION MATERIALS COMPANY, INC. TESTING	 One of the world's finest test tubes	 THERMOCYCLERS / ELECTROPHORESIS	 FINE LABORATORY GLASSWARE	 FINE LABORATORY GLASSWARE	 PHI METER / CONDUCTIVITY METER / TOSCAN	 COLOR MEASUREMENT / WATER TESTING
 UNIVERSAL OVENS / INCUBATORS / STERILIZERS / COOLED INCUBATORS / HEATING CABINETS	 TISSUE PROCESSOR / PARAFFIN EMBEDDING	 Brand Products	 Brand Products	 SOLID/LIQUID EXTRACTIONS • DISTILLATION SYSTEMS • DIGESTION SYSTEMS			

TELS.

731-9745 • 731-9746 • 731-1795 • 731-4974 FAX NO.: 742-2368

52 SCT. O.M. ALCARAZ COR. D. TUAZON STS., QUEZON CITY, METRO MANILA P.O. BOX 3886, MANILA, PHILIPPINES